Digital micromirror device projection printing system for meniscus tissue engineering

Shawn P. Grogan [a,b], Peter H. Chung [c], Pranav Soman [c], Peter Chen [a,d], Martin K. Lotz [b], Shaochen Chen [c], Darryl D. D'Lima [a,b,*]

[a] Shiley Center for Orthopaedic Research and Education at Scripps Clinic, 11025 North Torrey Pines Road, Suite 200, La Jolla, CA 92037, USA
[b] Department of Molecular and Experimental Medicine, The Scripps Research Institute, 10555 North Pines Road, MEM-161, La Jolla, CA 92037, USA
[c] Department of NanoEngineering, University of California, San Diego, La Jolla, CA 92093, USA
[d] Department of Engineering, University of California, San Diego, La Jolla, CA 92093, USA

ABSTRACT

Meniscus degeneration due to age or injury can lead to osteoarthritis. Although promising, current cell-based approaches show limited success. Here we present three-dimensional methacrylated gelatin (GelMA) scaffolds patterned via projection stereolithography to emulate the circumferential alignment of cells in native meniscus tissue. Cultured human avascular zone meniscus cells from normal meniscus were seeded on the scaffolds. Cell viability was monitored, and new tissue formation was assessed by gene expression analysis and histology after 2 weeks in serum-free culture with transforming growth factor $\beta 1$ (10 ng ml^{-1}). Light, confocal and scanning electron microscopy were used to observe cell–GelMA interactions. Tensile mechanical testing was performed on unseeded, fresh scaffolds and 2-week-old cell-seeded and unseeded scaffolds. 2-week-old cell–GelMA constructs were implanted into surgically created meniscus defects in an explant organ culture model. No cytotoxic effects were observed 3 weeks after implantation, and cells grew and aligned to the patterned GelMA strands. Gene expression profiles and histology indicated promotion of a fibrocartilage-like meniscus phenotype, and scaffold integration with repair tissue was observed in the explant model. We show that micropatterned GelMA scaffolds are non-toxic, produce organized cellular alignment, and promote meniscus-like tissue formation. Prefabrication of GelMA scaffolds with architectures mimicking the meniscus collagen bundle organization shows promise for meniscal repair. Furthermore, the technique presented may be scaled up to repair larger defects.

© 2013 Acta Materialia Inc. Published by Elsevier Ltd. All rights reserved.

1. Introduction

The meniscus has a role in stabilizing the knee joint and functions as a shock absorber which protects articular cartilage during walking and sporting activities. A meniscal tear is the most frequently recorded orthopedic diagnosis, and partial or total meniscectomy remains the most common orthopedic procedure [1]. The annual incidence of meniscal injuries in the USA is estimated to be between 600,000 and 850,000, with 90% resulting in meniscal surgery. The vast majority of these procedures involve partial, sub-total or total meniscectomy [2–4]. Untreated damaged or degenerate meniscus can lead to the development of osteoarthritis (OA). OA is the main cause of disability in the USA, affecting over 27,000,000 people [5]. Despite substantial developments in surgical techniques, instrumentation, and orthopedic devices, long-term clinical outcomes are unsatisfactory.

Partial meniscectomy, in which only the torn and damaged portions of the menisci are removed [6], is now the treatment of choice for meniscal tears that cannot be repaired. Partial meniscectomy effectively relieves the acute symptoms, such as pain, swelling, and locking of the knee. However, partial meniscectomy fails to prevent the onset of severe OA, which occurs on average 14 years after the original procedure [7,8].

Surgical attempts to repair the torn tissues are ineffective in the avascular zone and are associated with a re-rupture rate of 30% even in the vascular zone [4]. Furthermore, repairs deemed successful in the short term do not mitigate long-term degenerative changes and the onset of OA. The sequelae of meniscal injury and the clinical outcomes of meniscectomy or repair are significantly worse in patients over the age of 40 [9]. Despite major advances in surgical techniques and biomedical device development, a meta-analysis of 42 clinical studies found no difference in the incidence of radiographic OA after meniscal repair compared with partial or total meniscectomy [8].

To address this medical challenge an attempt to repair meniscus tears was the first logical step taken by many researchers. Biomaterials used to culture meniscus cells or stem cells for meniscus

repair include bioresorbable collagen matrices [10], which have been implanted in human patients with varied outcomes [11–13]. Fibrin alone or fibrin with added growth factors has been used to heal horizontal tears in human patients [14]. A recent report describes human meniscus cells seeded on a resorbable combination of polyglycolic acid (PGA) and hyaluronic acid in fibrin [15]. Polyurethane scaffolds possess sufficient mechanical properties with optimal interconnective macro-porosity to facilitate cell in-growth and differentiation [16]. Vicryl mesh scaffolds have also been used to repair bucket handle lesions in porcine meniscus [17]. A combination of human bone marrow-derived stem cells (hMSC) and a collagen scaffold was used in ovine meniscus explants showing promising integration [18]. Better integration was seen when the open/spongy scaffold structure was adjacent to the tissue. Devitalized meniscus has also been used to take advantage of the existing tissue architecture [19,20]. Although using the natural tissue may seem more promising for meniscus tears, a mature tissue scaffold without cells may not be ideal, and the availability of mensiscal tissue is also an issue.

A cell-seeded supportive scaffold system that emulates the structure and possesses the mechanical properties of native meniscus may aid in integrating and stabilizing the repair site and promote seamless repair. In the short term such an implanted cell-seeded scaffold should permit the cells to proliferate locally, migrate into the interface between the scaffold and native tissue, and secrete matrix components that integrate the scaffold.

Building structures mimicking native tissues can be accomplished using a number of nano- and micro-fabrication techniques, including melt molding, porogen leaching, gas foaming, phase separation, lamination, and fiber-based techniques [21–26]. More recently rapid prototyping techniques have been applied to biomaterial scaffold fabrication to refine the spatial complexity with which complex three-dimensional (3-D) physiological architectures can be replicated in vitro using laser ablation, microfluidics and 3-D printing [21,27–29]. In particular, projection stereolithography (PSL) or digital micromirror device (DMD) microfabrication, which uses an array of digitally controlled micromirrors to fabricate 3-D scaffolds layer by layer via a reflective photomask, is a promising technique. Because photomasks can be easily changed on demand the PSL approach is attractive due to its relative speed and flexibility compared with other photopatterning techniques [27,30–34]. This technique allows the rapid assembly of cell-responsive hydrogels that feature highly specified complex 3-D geometries with micrometer resolution.

In this study we demonstrate the feasibility of combining cell therapy, photocrosslinkable hydrogels, and digital micromirror device projection stereolithography (DMD PSL) microfabrication to produce graft tissue for implantation and integration into a meniscus tear. We fabricated scaffolds using a hydrolyzed form of collagen type I, the major structural component of the meniscal tissue, to provide structure and function similar to the surrounding native meniscus tissue. We confirmed cell compatibility (viability), observed cell interactions with the patterned scaffold (attachment and organization), characterized the mechanical properties of the scaffold before and after cell seeding, demonstrated new human meniscus tissue formation, and explored the potential for cell-seeded GelMA scaffolds to integrate with native meniscus tissue in an ex vivo human meniscus defect.

2. Methods

2.1. Tissue procurement

Normal human meniscus (medial and lateral) was obtained from tissue banks (approved by Scripps institutional review board), from six donors (age range 18–61 years, mean age 37.2 ± 17.5, one female, five males). A previously reported macroscopic and histologic grading system was used to select normal menisci [35].

2.2. Cell isolation and monolayer culture

Meniscus tissue was cut to isolate the avascular (inner two thirds) and vascular (outer one third) regions. The separated tissues were subjected to collagenase digestion as previously described [36], except that digestion over 5–6 h. The digested tissues were filtered through 100 μm cell strainers (BD Biosciences, San Jose, CA) and seeded in monolayer culture in Dulbecco's modified Eagle's medium (DMEM) (Mediatech Inc., Manassas, VA) supplemented with 10% calf serum (Omega Scientific Inc., Tarzana, CA) and penicillin/streptomycin/gentamycin (Invitrogen, Carlsbad, CA).

2.3. Synthesis of methacrylated gelatin incorporating CaCO$_3$ particles (GelMA)

Gelatin methacrylate was prepared as described previously [37]. Briefly, porcine skin gelatin (Sigma-Aldrich, St Louis, MO) was dissolved at 10% w/v in phosphate-buffered saline (PBS) (Gibco/Life Technologies, Grand Island, NY) at 60 °C and stirred for 1 h. Methacrylic anhydride (Sigma–Aldrich) was added at a rate of 0.5 ml min^{-1} at 50 °C to achieve a final concentration of 7.5 vol.% and allowed to react for 2 h. The product was dialyzed against dH$_2$O at 40 °C for 1 week using dialysis tubing (molecular weight cut-off 12–14 kDa, Spectrum Laboratories). Finally, the solution was filtered (0.2 μm), frozen overnight (−80 °C), and lyophilized for 1 week. The final product was stored at −80 °C until further preparation.

To aid mechanical stability during fabrication CaCO$_3$ particles were incorporated into the final GelMA macromer solution. First, a 3% w/v macromer solution was prepared by adding GelMA to pre-warmed PBS (60 °C) and stirring until fully dissolved. An equal volume of 1.65 M CaCl$_2$ in PBS was added to the GelMA solution until thoroughly mixed. 1.65 M Na$_2$CO$_3$ in PBS (volume equivalent to the CaCl$_2$ solution) was added dropwise, and the mixture was stirred at 40 °C for 24 h. After allowing the mixture to settle, excess supernatant was removed to produce a 1.5% w/v GelMA concentration. Additional GelMA was then added to reach a 15% w/v concentration. Photoinitiator Irgacure 2959 (1% w/v, Ciba/BASF, Florham Park, NJ), UV absorber 2-hydroxy-4-methoxy-benzphenone-5-sulfonic acid (0.1% w/v), and UV quencher TEMPO (0.01% w/v, Sigma–Aldrich) were added sequentially until fully dissolved.

To determine the extent of methacrylate conversion (i.e. the degree of modification of ε-amine groups on lysines in gelatin), the 2,4,6-trinitrobenzenesulfonic acid solution (TNBS) assay as described by Habeeb was used [38]. The percentage amine substitution was calculated using the formula:

Percentage substitution

= [1 − (absorbance of the methacrylated protein

− absorbance of the blank)/(absorbance of the native protein

− absorbance of the blank)] × 100%.

2.4. Digital micromirror device (DMD) projection stereolithography system

GelMA scaffolds were fabricated using a modified version of a DMD projection stereolithography (PSL) system described elsewhere [33]. The fabrication platform (Fig. 1A) comprises a DMD system (1920 × 1080 Discovery 4000, Texas Instruments), a servo-controlled stage (CMA-25-CCCL & ESP300, Newport), a UV light source (200 W, S2000, EXFO), a UV grade projection lens (Edmond Optics), and a replaceable glass coverslip window

(No. 1, 22 × 22 mm, Fisher) onto which the UV light is focused. Using a computer, specified patterns for each layer of the scaffold are loaded onto the DMD, which consists of a 1920 × 1080 pixel array of micro-mirrors. These patterns provide a series of reflective photomasks that can be changed on demand. During fabrication UV light is reflected off the DMD and focused via the projection lens onto the photocurable GelMA solution, which is placed between the glass coverslip and the

servo-controlled stage. The GelMA solution is selectively cured in the regions specified by the DMD array, with the height of each cured layer defined by the distance between the glass coverslip and the servo-controlled stage. The glass coverslip is coated with Krytox 157 FSH oil (DuPont, Wilmington, DE) to aid in release of the polymerized scaffold layer from the coverslip surface after UV exposure. The glass coverslip is replaced after fabrication of each layer.
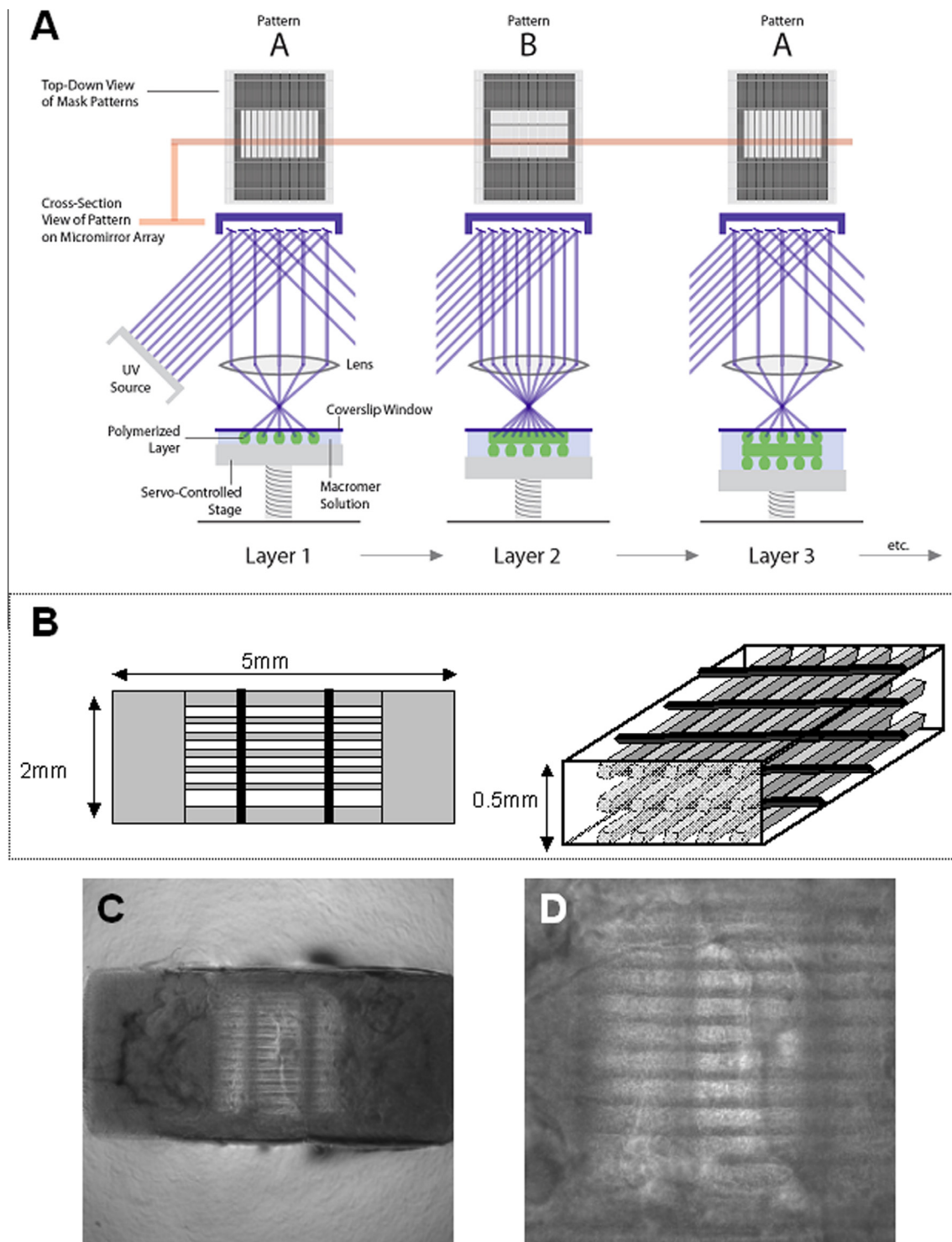

Fig. 1. (A) Overview of the digital micromirror device projection stereolithography (DMD PSL) system used to make the GelMA scaffolds and design of the scaffold. (B) Cartoon showing the basic scaffold design pattern. (C, D) Phase contrast micrograph images of GelMA scaffolds produced. (C) 4×; (D) 10×.

2.5. Layer by layer scaffold fabrication

Fig. 1A shows the scaffold fabrication process. The photocurable GelMA/CaCO$_3$ mixture was stirred at 35 °C during fabrication. CaCO$_3$ aids in maintaining better structural integrity of the scaffold structure during fabrication and is removed after fabrication. After placing a drop of the GelMA/CaCO$_3$ on the stage the distance between the glass coverslip and the stage was adjusted initially to 100 µm for fabrication of the first layer. The UV image was then projected onto the glass coverslip for 8 s at a power of 50 mW cm^{-2}. After polymerization of the first layer the stage was moved down to release the scaffold from the glass coverslip. The scaffold and stage were washed with PBS, a new drop of Gel-MA/CaCO$_3$ was added to the top of the scaffold, and the coated glass coverslip was replaced. After changing the DMD image the stage was moved to the new position (100 µm), and the next layer was exposed to UV light. These steps were repeated for all five layers of the scaffold to construct the final layered 3-D structure approximately 500 µm high. Each longitudinal rod is 20 µm wide and ~1800 µm long. These dimensions were chosen to represent the bundles of collagen fibrils that run circumferentially in the main central portion of the meniscus. The spacing between the rods (100 µm) was at the lower end of the pore diameter required for cellular infiltration. The supporting transverse rods are 50 µm wide and ~1730 µm long. These were constructed to provide stability and link the longitudinal layers. The distance between the glass coverslip and the stage was increased for each subsequent layer by increments of 100 µm, and the images were projected using the same intensity and duration as the initial layer. Fig. 1A illustrates the specific image sequences used to generate the layered scaffold resembling a "log pile" to replicate the dominant structure of the circumferentially oriented collagen fibers in native menisci.

After fabrication the complete scaffold was removed from the stage using a scalpel, placed in a bath of 10 mM HCl for 30 min to dissolve the incorporated CaCO$_3$, and thoroughly rinsed with PBS. In total the fabrication time for each five layer scaffold was approximately 35–40 min, including scaffold projection, washing and removal of the CaCO$_3$.

2.6. Cell seeding and 3-D culture

The GelMA scaffolds were placed in cell culture inserts (8 µm, BD Biosciences) inserted into 24-well plates and maintained in PBS until ready for cell seeding. To seed the cells the PBS was removed and the cells were seeded at a density of 1×10^6 cells ml^{-1} in 50 µl of medium (50,000 cells per scaffold). The 50 µl cell suspension remained on the scaffold for 20 min to permit cell attachment before medium was added to the outer well. The medium moved up through the membrane at the base of the cell culture insert to bathe the cell-seeded scaffold. However, higher volumes of medium were avoided since many scaffolds floated, which may reduce cell migration into the scaffold from the surrounding membrane.

The medium used in 3-D culture consisted of DMEM (Cellgro, Manassas, VA), $1 \times$ ITS + (Sigma) (i.e. 10 mg ml^{-1} insulin, 5.5 mg ml^{-1} transferrin, 5 ng ml^{-1} selenium, 0.5 mg ml^{-1} bovine serum albumin, 4.7 mg ml^{-1} linoleic acid), 1.25 mg ml^{-1} human serum albumin (Bayer, Leverkusen, Germany), 100 nM dexamethasone (Sigma), 0.1 mM ascorbic acid 2-phosphate (Sigma), and penicillin/streptomycin/gentamycin (Gibco, Carlsbad, CA) [39]. This mix was filter sterilized through a 0.22 µm filter. To stimulate new meniscus tissue formation transforming growth factor (TGF) β1 (10 ng ml^{-1}) was added to the medium immediately prior to use for all conditions.

2.7. Cell viability

The viability of cells cultured on GelMA scaffolds was observed using a live/dead kit consisting of calcein-AM and ethidium homerdimer-1 (Invitrogen) and a confocal laser microscope (LSM-510, Zeiss, Jena, Germany) as previously demonstrated [40].

2.8. Histology and immunohistochemistry

2-week-old GelMA scaffolds seeded with meniscus fibrochondrocytes were cryofixed in tissue Tech (Info) on dry ice and cryosectioned at ~7 µm thick. The sections were stained with hematoxylin and eosin (H&E) and safranin O-fast green. To detect collagen type I by immunohistochemistry cut sections were fixed in 4% formaldehyde for 10 min at room temperature, treated with hyaluronidase for 2 h [41] and incubated with primary antibodies against collagen type I (clone I-8H5, MP Biomedicals, Santa Ana, CA) at 10 µg ml^{-1}. Secondary antibody staining and detection procedures were as previously described [42]. Isotype controls were used to control for non-specific staining.

2.9. RNA isolation and RT polymerase chain reaction (PCR)

Total RNA was isolated from the GelMA constructs using a RNA-easy mini kit (Qiagen, Hilden, Germany) and first strand cDNA was produced according to the manufacturer's protocols (Applied Biosystems, Foster City, CA). Quantitative RT-PCR was performed using TaqMan® gene expression reagents. COL1A1, aggrecan, Sox9 and GAPDH were detected using Assays-on-Demand™ primer/probe sets (Applied Biosystems). GAPDH was used to normalize gene expression levels using the recommended ΔC_t method, and fold-change was calculated using the $2^{-\Delta\Delta Ct}$ formula [43].

2.10. Mechanical testing

The tensile strength of the GelMA construct along the axis of the "log piles" was assessed using a custom built device consisting of two miniature brushless servo actuators (SMAC, Carlsbad, CA) and one 50 g load cell (FUTEK, Irvine, CA). The scaffold was secured between two coverslips (100 µm thick) using a cyanoacrylate glue. The base coverslip was glued down to a stainless steel block as an anchor, while the upper coverslip was attached to a steel plunger having a flat surface which served as the actuator to pull the scaffolds (Supplementary Fig. 1). LabVIEW (National Instruments, Austin, TX) software was employed for movement control and data acquisition on a laptop. The gel height was measured using electronic calipers. The force to pull the gel to breaking was monitored and recorded. The Young's modulus was calculated as previously reported [44].

2.11. Scanning electron microscopy (SEM)

Avascular meniscus cells cultured on GelMA for 14 days were washed with PBS and fixed with 2.5% w/v glutaraldehyde (Sigma, USA) for 1 h. After fixation they were washed three times with PBS for 10 min each wash. The scaffold was dehydrated in a graded series of ethanol (50%, 70%, and 90%) for 30 min each and left in 100% ethanol for 24 h at −20 °C. The scaffold was dried in a critical point dryer (EMS 850, Electron Microscopy Science Co., Chelmsford, MA) and then surface metalized by sputter coating with iridium for SEM examination (XL30, FEI Co., Hillsboro, OR).

2.12. Organ culture repair model

Sections of human meniscus from one donor (18-year-old male) were cultured in medium in 6-well plates for 2–3 days following

processing. One full thickness defect per tissue section was created with a scalpel parallel to the circumferential direction to simulate a longitudinal tear. Two-week-old cultured GelMA scaffolds with avascular meniscus fibrochondrocytes (22-year-old male) was placed in the defect with the "log piles" oriented parallel to the circumferential collagen bands. The tissues were maintained in differentiation medium (8 ml well^{-1}) for 3 weeks (with medium changes every 2–3 days) and processed for histology to examine scaffold/cell integration with the native tissue and for new tissue development.

3. Results

3.1. Human meniscus cells are organized by the GelMA scaffold architecture

Following 2 weeks culture human avascular meniscus cells seeded onto GelMA scaffolds remained viable and were aligned along the "log pile" strands of GelMA (Fig. 2B and C). Scanning electron micrographs showed the alignment and intimate interaction between the meniscus cells and GelMA scaffold (Fig. 2D–E).

3.2. Meniscus-like new tissue is formed on GelMA scaffolds

The Young's modulus of the scaffold was 14.3 ± 4.0 kPa (Fig. 3). No change in mechanical properties was detected over time in culture medium alone or when seeded with cells (Fig. 3). The extent of methacrylation was calculated to be greater than 90%, with a mass swelling ratio of 5.9, indicating that the mechanical properties of the GelMA were close to maximum [45]. Histological analysis indicated the formation of multilayered and aligned new tissue (Fig. 4A–E). This tissue lacked glycosaminoglycans (GAG), as seen in the safranin-O staining (Fig. 4D), yet contained collagen type I (Fig. 4E), which complements the gene expression profile of high COL1A1 mRNA levels (Fig. 4F). Increased Sox9 also indicates redifferentiation to the meniscus phenotype (data shown as gene expression relative to monolayer cultured cells).

3.3. Cell seeded GelMA scaffolds integrate with native meniscus tissue

Human meniscus cells seeded on GelMA scaffolds for 2 weeks were placed in surgically created defects in meniscus tissue (Fig. 5A and B). After 3 weeks of free swelling culture in 6-well plates histological analysis revealed the generation of new tissue between the implanted scaffolds and the native tissue (Fig. 5C–N). The new tissue is multilayered (Fig. 5D) and shows virtually no GAG staining (Fig. 5G).

4. Discussion

Digital micromirror device projection stereolithography (DMD PSL) to produce specified micropatterns is a useful means to create scaffolds that emulate the structure of native tissue architectures. We have shown that the micropatterned GelMA scaffolds produced in this study maintain human meniscus cell viability without cytotoxic effects, produce an organized cellular alignment in response to the scaffold microstructure, and promote the formation of meniscus-like tissues. Prefabrication of organized GelMA scaffolds with an architecture mimicking the meniscus collagen bundle organization shows promise for the repair of meniscal tears, as demonstrated by the formation of integrated new tissue in the ex vivo meniscus defect model. Scaling up of this approach may be useful to repair larger defects.

To our knowledge scaffolds employing DMD microfabrication have not been used for meniscus tissue engineering nor for meniscal defect repair. Specific combinations of GelMA and microengineering have been tested with various cell types and to direct specific cell patterns, including fibroblasts, myoblasts, endothelial
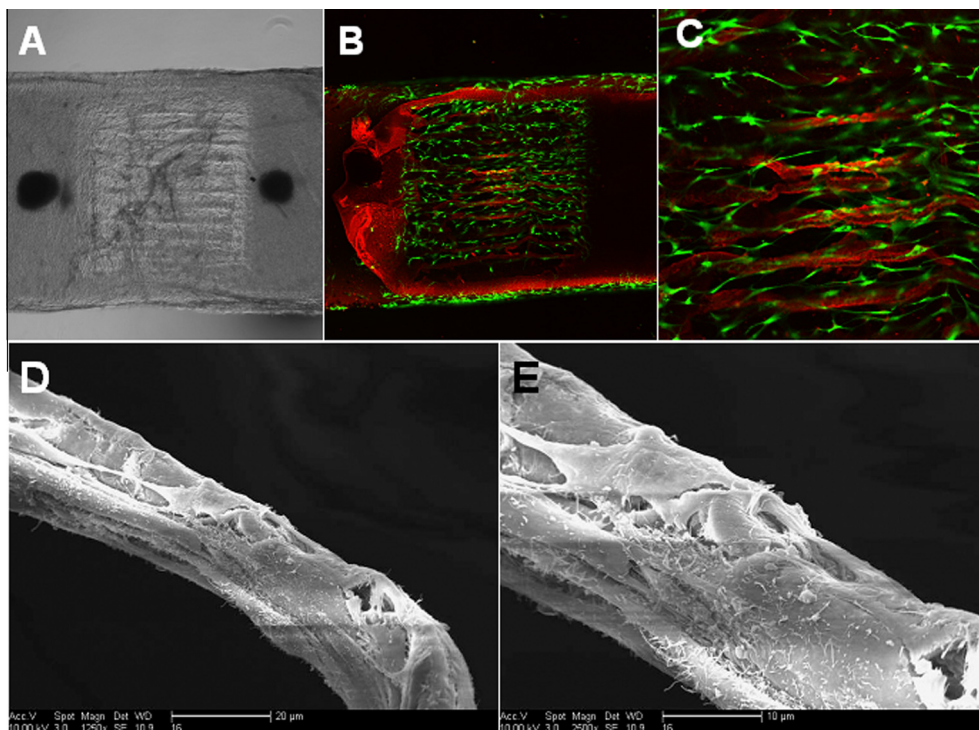

Fig. 2. Cell viability and interaction with the GelMA scaffold. (A) Phase contrast image of a meniscus cell-seeded GelMA scaffold (4×). (B) Confocal image showing live cells (green) attached to GelMA "log piles" (composite of a 3 × 3 scan at 10× magnification). (C) Center region confocal image scan (10×). (D, E) Scanning electron micrographs of the cell–GelMA interaction. (D) 1250×; (E) 2500×.
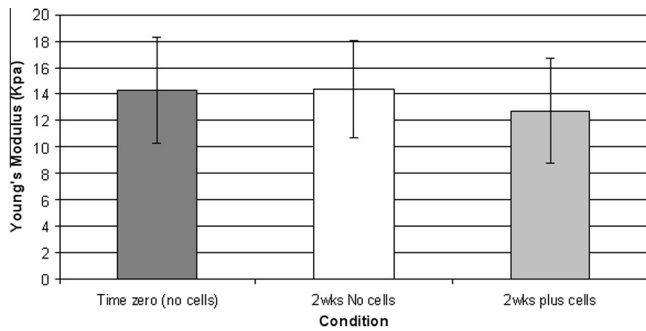
Fig. 3. Measurement of Young's modulus. Mean ± SD of the calculated Young's modulus (kPa) for scaffolds at time zero and after 2 weeks in culture medium, with and without cells.

cells, cardiac stem cells [37], human umbilical vein endothelial cells [46], NIH-3T3 cells and human mesenchymal stem cells [47]. Spatial organization of embryoid bodies have been made in GelMA [48] and Aubin et al. [37] demonstrated that GelMA hydrogels could be useful in creating complex, cell-responsive microtissues, such as endothelialized microvasculature. Other studies using projection printing technologies have been used with numerous different cell types [1,31,34,49,50]. Combined application of GelMA hydrogels and dielectrophoresis (DEP) is another method for creating highly complex microscale scaffold/tissue constructs using myoblasts or endothelial cells [47].

The new tissue produced on the GelMA scaffolds appeared to be fibrocartilage-like with high expression of COL1A1 (mRNA and protein), as reported elsewhere for native [51–54] and engineered meniscus [15]. Similarly to the vascular region, we did not observe increased aggrecan expression or detect COL2A1. The increase in Sox9 expression indicates that longer term cultures may be needed to induce expression of COL2A1 and aggrecan [55]. Mechanical stimulation [27,56,57], hypoxic conditions [58,59], or other growth factors such as TGFβ3 [60,61], insulin-like growth factor 1 [62] and fibroblast growth factor 2 [62,63] might perhaps enhance tissue generation relative to the non-mechanical loading, normoxic conditions and TGFβ1 used in this current study. Sox9 expression may also indicate the beginning of a shift towards a more "chondrocyte-like" phenotype that is characteristic of the avascular region [64–66].

The in vitro model developed here has demonstrated the potential for cell-seeded GelMA to integrate with native tissues. The open structure of the GelMA scaffold mimicking native collagen fiber bundles may also have encouraged integration. Pabbruwe et al. [18] seeded MSC in collagen scaffolds which they implanted into ovine meniscus explants. Better integration was seen with scaffolds when the open/spongy structure was adjacent to the tissue. As discussed, the new tissue formed on GelMA may be more reminiscent of repair in the vascular zone of meniscus. Vascular zone tissue transplanted into avascular zone defects was shown to better integrate with the surrounding avascular tissue compared with
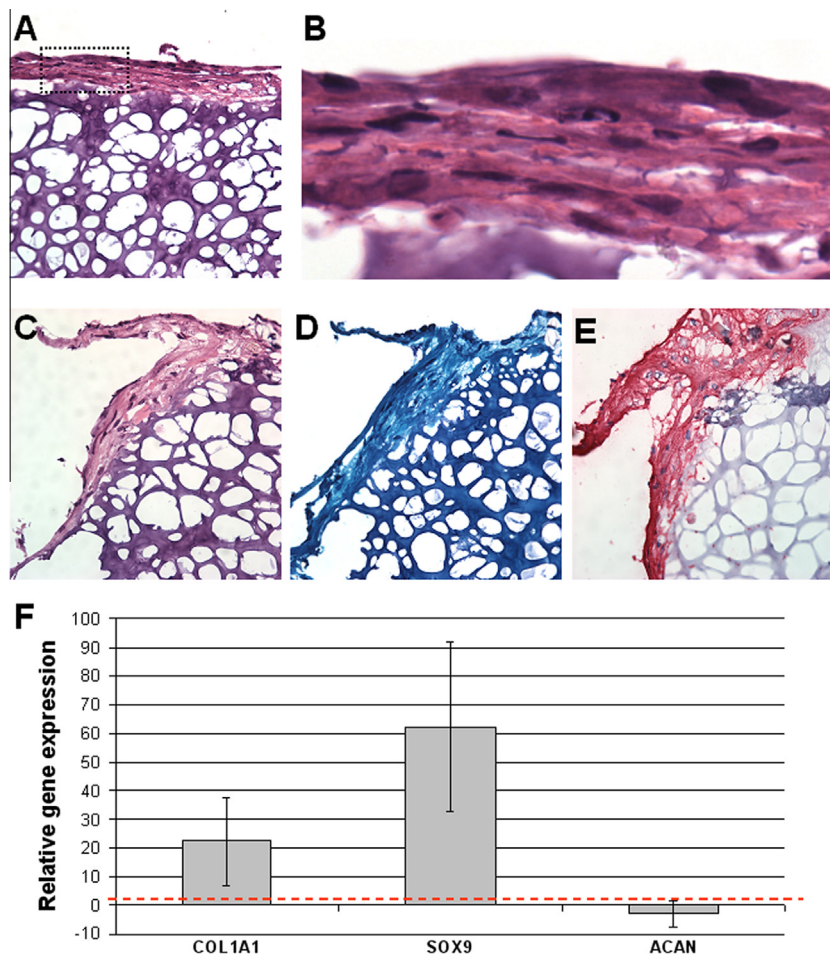

Fig. 4. Histology, immunohistochemistry (IHC) and RT-PCR. (A) H&E stain. (B) Production of cell layers on the GelMA scaffold. (C) H&E stain. (D) Safranin O-fast green stain. (E) Type I collagen IHC (red color). (F) Gene expression profile of meniscus cells cultured on GelMA for 2 weeks relative to monolayer expanded cell gene expression values denoted by red dotted line. (A), (C–E) 40×.
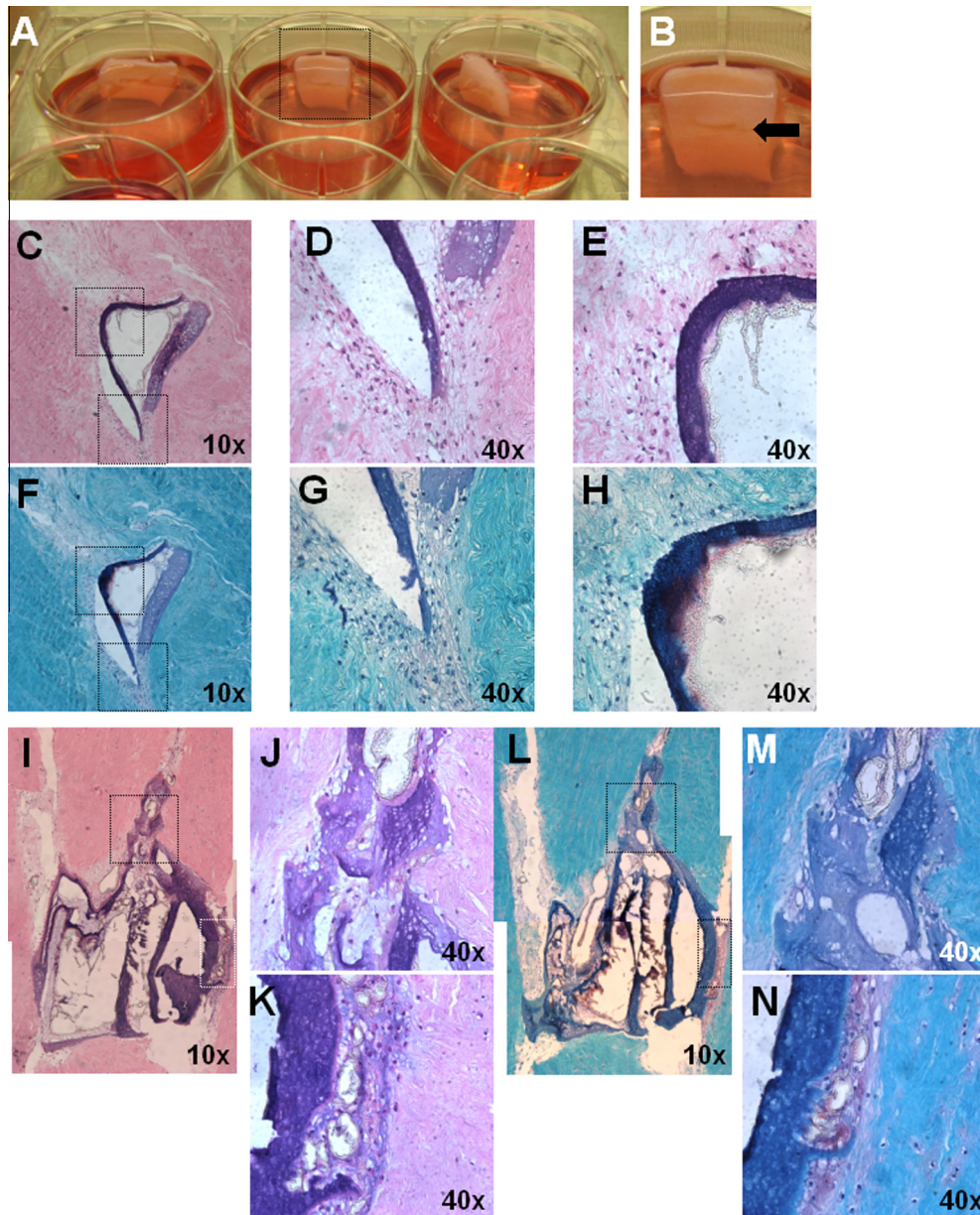
Fig. 5. Human meniscus ex vivo repair model. (A) Defects were surgically produced in human meniscus tissue and 2-week-old meniscus cell-seeded GelMA scaffolds were inserted and cultured for a further 4 weeks. (B) A closer view of the defect. (C–N) Histology of two different defects showing areas of new tissue formation that integrated with the surrounding meniscus tissue. (C–E, I–K) H&E stain; (F–H, L–N) safranin O-fast green stain. Magnifications shown on each panel.

re-implanted avascular zone tissue [50]. Combining GelMA with other biocompatible materials, like fibrin glue, may further promote defect repair. Synovial tissue grafts were implanted into human meniscal lesions and were found to integrate better compared with fibrin glue in terms of cell infiltration and improved tissue formation in the defect [67]. Therefore synoviocytes might be useful as they are more readily available than meniscal cells.

The use of a DMD PSL system allowed the formation of 3-D GelMA scaffolds with aligned gelatin fibers mimicking the collagen bundles of native meniscal tissue. In contrast to other 3-D patterning approaches, DMD projection printing offers advantages in terms of speed, flexibility, and scalability. Generally the use of photopolymer-based approaches allows the production of complex patterns that may be difficult to construct using cast molding and electrospinning. While 3-D plotting can fabricate sophisticated architectures, the approach is often limited by its slow processing

speed and the low mechanical strength of the final scaffolds [21]. Micromirror arrays allow the use of rapidly interchangeable photomasks during the layer by layer fabrication process, providing more rapid construction of the patterned substrates. This ability to generate a complete layer in one simultaneous exposure confers improved scalability to the PSL platform. Additionally, as each layer is created in a discrete step with replenishment of the prepolymer, a multilayered composite 3-D structure can be easily created by exchanging the prepolymer composition at various points. The projection printing method is limited mainly by its lower resolution (~5 μm) compared with two photon polymerization methods, as well as by post-curing steps that may be necessary to provide additional mechanical integrity. Because polymerization of each additional layer further irradiates the preceding layers, cumulative exposure and thereby crosslinking density may vary throughout the layers if the prepolymer solution is not properly

rinsed out and replenished for each step. Additionally, not all bio-polymers may be amenable to the modifications necessary to make them photopolymerizable [15].

Despite the favorable interaction of human meniscus cells with the GelMA scaffolds (low toxicity and new tissue formation), we noted a number of less favorable outcomes. Promising integration between the new tissue and the native meniscus tissue was observed in an ex vivo defect model, however, the relatively poor tensile mechanical properties of the existing GelMA scaffolds may not withstand the mechanical forces in the in vivo knee environment. The stiffness of the DMD fabricated scaffold was lower than reported for solid GelMA, reflecting the effect of the spaces between the "logs" [45]. The stiffness to withstand clinically relevant forces is much higher ($\sim$150 kPA) and not likely to be achievable with GelMA [68]. To overcome this variable other hydrogels possessing tunable mechanical properties, such as polyethylene glycol [30,49,69] or alginate [27], could be used employing a DMD PSL system. We also noted an issue with uniform cell seeding. The majority of seeded cells remained on the surface of the GelMA construct. While using the projected printing technologies described here it would be conceivable to accurately incorporate a chemo-attractant molecule, like platelet-derived growth factor [70] into the internal layers of the scaffold to encourage better scaffold cell infiltration.

5. Conclusions

In summary, we have demonstrated the utility of using DMD PSL with GelMA for the rapid production of organized scaffolds that emulate meniscus collagen bundles, which directed cell alignment and supported the development of viable new meniscus tissue in vitro. Moreover, we have shown the promise of using these scaffolds to repair meniscus lesions in an ex vivo organ culture model. Scaling up of this approach may be useful to repair larger defects.

Acknowledgements

Appendix A. Figures with essential colour discrimination

Certain figures in this article, particularly Figs. 1,2, 4 and 5 are difficult to interpret in black and white. The full colour images can be found in the on-line version, at http://dx.doi.org/10.1016/j.actbio.2013.03.020.

Appendix B. Supplementary data

Supplementary data associated with this article can be found, in the online version, at http://dx.doi.org/10.1016/j.actbio.2013.03.020.

References

[1] Garrett WE, Swiontkowski MF, Weinstein JN, Callaghan J, Rosier RN, Berry DJ, et al. American board of orthopaedic surgery practice of the orthopaedic surgeon: Part-II. Certification examination case mix. J Bone Joint Surg Am 2006;88:660–7.

[2] Fetzer GB, Spindler KP, Amendola A, Andrish JT, Bergfeld JA, Dunn WR, et al. Potential market for new meniscus repair strategies: evaluation of the MOON cohort. J Knee Surg 2009;22:180–6.

[3] Ford GM, Hegmann KT, White GL, Holmes EB. Associations of body mass index with meniscal tears. Am J Prev Med 2005;28:364–8.

[4] Makris EA, Hadidi P, Athanasiou KA. The knee meniscus: structure–function, pathophysiology, current repair techniques, and prospects for regeneration. Biomaterials 2011;32:7411–31.

[5] Lawrence RC, Felson DT, Helmick CG, Arnold LM, Choi H, Deyo RA, et al. Estimates of the prevalence of arthritis and other rheumatic conditions in the United States. Part II. Arthritis Rheum 2008;58:26–35.

[6] Gillquist J, Hamberg P, Lysholm J. Endoscopic partial and total meniscectomy. A comparative study with a short term follow up. Acta Orthop Scand 1982;53:975–9.

[7] Englund M, Roos EM, Roos HP, Lohmander LS. Patient-relevant outcomes fourteen years after meniscectomy: influence of type of meniscal tear and size of resection. Rheumatology (Oxford) 2001;40:631–9.

[8] Lohmander LS, Englund PM, Dahl LL, Roos EM. The long-term consequence of anterior cruciate ligament and meniscus injuries: osteoarthritis. Am J Sports Med 2007;35:1756–69.

[9] Barrett GR, Field MH, Treacy SH, Ruff CG. Clinical results of meniscus repair in patients 40 years and older. Arthroscopy 1998;14:824–9.

[10] Reguzzoni M, Manelli A, Ronga M, Raspanti M, Grassi FA. Histology and ultrastructure of a tissue-engineered collagen meniscus before and after implantation. J Biomed Mater Res B Appl Biomater 2005;74:808–16.

[11] Ronga M, Grassi FA, Manelli A, Bulgheroni P. Tissue engineering techniques for the treatment of a complex knee injury. Arthroscopy 2006;22:576.e1–3.

[12] Stone KR, Steadman JR, Rodkey WG, Li ST. Regeneration of meniscal cartilage with use of a collagen scaffold. Analysis of preliminary data. J Bone Joint Surg Am 1997;79:1770–7.

[13] Zaffagnini S, Giordano G, Vascellari A, Bruni D, Neri MP, Iacono F, et al. Arthroscopic collagen meniscus implant results at 6 to 8 years follow up. Knee Surg Sports Traumatol Arthrosc 2007;15:175–83.

[14] Kamimura T, Kimura M. Repair of horizontal meniscal cleavage tears with exogenous fibrin clots. Knee Surg Sports Traumatol Arthrosc 2011;19:1154–7.

[15] Freymann U, Endres M, Neumann K, Scholman HJ, Morawietz L, Kaps C. Expanded human meniscus-derived cells in 3-D polymer-hyaluronan scaffolds for meniscus repair. Acta Biomater 2012;8:677–85.

[16] Buma P, Ramrattan NN, van Tienen TG, Veth RP. Tissue engineering of the meniscus. Biomaterials 2004;25:1523–32.

[17] Weinand C, Peretti GM, Adams SB, Randolph MA, Savvidis E, Gill TJ. Healing potential of transplanted allogeneic chondrocytes of three different sources in lesions of the avascular zone of the meniscus: a pilot study. Arch Orthop Trauma Surg 2006;126:599–605.

[18] Pabbruwe MB, Kafienah W, Tarlton JF, Mistry S, Fox DJ, Hollander AP. Repair of meniscal cartilage white zone tears using a stem cell/collagen-scaffold implant. Biomaterials 2010;31:2583–91.

[19] Peretti GM, Gill TJ, Xu JW, Randolph MA, Morse KR, Zaleske DJ. Cell-based therapy for meniscal repair: a large animal study. Am J Sports Med 2004;32:146–58.

[20] Sandmann GH, Eichhorn S, Vogt S, Adamczyk C, Aryee S, Hoberg M, et al. Generation and characterization of a human acellular meniscus scaffold for tissue engineering. J Biomed Mater Res A 2009;91:567–74.

[21] Billiet T, Vandenhaute M, Schelfhout J, Van Vlierberghe S, Dubruel P. A review of trends and limitations in hydrogel-rapid prototyping for tissue engineering. Biomaterials 2012;33:6020–41.

[22] Dvir T, Timko BP, Kohane DS, Langer R. Nanotechnological strategies for engineering complex tissues. Nat Nanotechnol 2011;6:13–22.

[23] Ifkovits JL, Burdick JA. Review: photopolymerizable and degradable biomaterials for tissue engineering applications. Tissue Eng 2007;13:2369–85.

[24] Kim HN, Kang DH, Kim MS, Jiao A, Kim DH, Suh KY. Patterning methods for polymers in cell and tissue engineering. Ann Biomed Eng 2012;40:1339–55.

[25] Norman JJ, Desai TA. Methods for fabrication of nanoscale topography for tissue engineering scaffolds. Ann Biomed Eng 2006;34:89–101.

[26] Subia B, Kundu J, Kundu SC. Biomaterial scaffold fabrication techniques for potential tissue engineering applications. In: Eberli D, editor. Tissue engineering. InTech; 2010.

[27] Baker BM, Shah RP, Huang AH, Mauck RL. Dynamic tensile loading improves the functional properties of mesenchymal stem cell-laden nanofiber-based fibrocartilage. Tissue Eng A 2011;17:1445–55.

[28] Melchels FP, Feijen J, Grijpma DW. A review on stereolithography and its applications in biomedical engineering. Biomaterials 2010;31:6121–30.

[29] Zervantonakis IK, Kothapalli CR, Chung S, Sudo R, Kamm RD. Microfluidic devices for studying heterotypic cell–cell interactions and tissue specimen cultures under controlled microenvironments. Biomicrofluidics 2011;5:13406.

[30] Fozdar DY, Soman P, Lee JW, Han LH, Chen S. Three-dimensional polymer constructs exhibiting a tunable negative Poisson's ratio. Adv Funct Mater 2011;21:2712–20.

[31] Han LH, Mapili G, Chen SC, Roy K. Projection microfabrication of three-dimensional scaffolds for tissue engineering. J Manuf Sci Eng 2008; 130:021005.

[32] Mapili G, Lu Y, Chen S, Roy K. Laser-layered microfabrication of spatially patterned functionalized tissue-engineering scaffolds. J Biomed Mater Res B Appl Biomater 2005;75:414–24.

[33] Suri S, Han LH, Zhang W, Singh A, Chen S, Schmidt CE. Solid freeform fabrication of designer scaffolds of hyaluronic acid for nerve tissue engineering. Biomed Microdevices 2011;13:983–93.

[34] Zhang AP, Qu X, Soman P, Hribar KC, Lee JW, Chen S, et al. Rapid fabrication of complex 3D extracellular microenvironments by dynamic optical projection stereolithography. Adv Mater 2012;24:4266–70.

[35] Pauli C, Grogan SP, Patil S, Otsuki S, Hasegawa A, Koziol J, et al. Macroscopic and histopathologic analysis of human knee menisci in aging and osteoarthritis. Osteoarthritis Cartilage 2011;19:1132–41.

[36] Blanco FJ, Ochs RL, Schwarz H, Lotz M. Chondrocyte apoptosis induced by nitric oxide. Am J Pathol 1995;146:75–85.

[37] Aubin H, Nichol JW, Hutson CB, Bae H, Sieminski AL, Cropek DM, et al. Directed 3D cell alignment and elongation in microengineered hydrogels. Biomaterials 2010;31:6941–51.

[38] Habeeb AF. Determination of free amino groups in proteins by trinitrobenzenesulfonic acid. Anal Biochem 1966;14:328–36.

[39] Barbero A, Grogan S, Schafer D, Heberer M, Mainil-Varlet P, Martin I. Age related changes in human articular chondrocyte yield, proliferation and post-expansion chondrogenic capacity. Osteoarthritis Cartilage 2004;12:476–84.

[40] Grogan SP, Aklin B, Frenz M, Brunner T, Schaffner T, Mainil-Varlet P. In vitro model for the study of necrosis and apoptosis in native cartilage. J Pathol 2002;198:5–13.

[41] Roberts S, Menage J, Sandell LJ, Evans EH, Richardson JB. Immunohistochemical study of collagen types I and II and procollagen IIA in human cartilage repair tissue following autologous chondrocyte implantation. Knee 2009;16:398–404.

[42] Grogan SP, Miyaki S, Asahara H, D'Lima DD, Lotz MK. Mesenchymal progenitor cell markers in human articular cartilage: normal distribution and changes in osteoarthritis. Arthritis Res Ther 2009;11:R85.

[43] Livak KJ, Schmittgen TD. Analysis of relative gene expression data using real-time quantitative PCR and the $2(-\text{delta delta }C(T))$ method. Methods 2001;25:402–8.

[44] Korhonen RK, Laasanen MS, Toyras J, Rieppo J, Hirvonen J, Helminen HJ, et al. Comparison of the equilibrium response of articular cartilage in unconfined compression, confined compression and indentation. J Biomech 2002;35:903–9.

[45] Nichol JW, Koshy ST, Bae H, Hwang CM, Yamanlar S, Khademhosseini A. Cell-laden microengineered gelatin methacrylate hydrogels. Biomaterials 2010;31:5536–44.

[46] Gauvin R, Chen YC, Lee JW, Soman P, Zorlutuna P, Nichol JW, et al. Microfabrication of complex porous tissue engineering scaffolds using 3D projection stereolithography. Biomaterials 2012;33:3824–34.

[47] Ramon-Azcon J, Ahadian S, Obregon R, Camci-Unal G, Ostrovidov S, Hosseini V, et al. Gelatin methacrylate as a promising hydrogel for 3D microscale organization and proliferation of dielectrophoretically patterned cells. Lab Chip 2012;12:2959–69.

[48] Qi H, Du Y, Wang L, Kaji H, Bae H, Khademhosseini A. Patterned differentiation of individual embryoid bodies in spatially organized 3D hybrid microgels. Adv Mater 2010;22:5276–81.

[49] Curley JL, Jennings SR, Moore MJ. Fabrication of micropatterned hydrogels for neural culture systems using dynamic mask projection photolithography. J Vis Exp 2011.

[50] Itoga K, Yamato M, Kobayashi J, Kikuchi A, Okano T. Cell micropatterning using photopolymerization with a liquid crystal device commercial projector. Biomaterials 2004;25:2047–53.

[51] Cheung HS. Distribution of type I, II, III and V in the pepsin solubilized collagens in bovine menisci. Connect Tissue Res 1987;16:343–56.

[52] Eyre DR, Wu JJ. Collagen of fibrocartilage: a distinctive molecular phenotype in bovine meniscus. FEBS Lett 1983;158:265–70.

[53] Gao J. Immunolocalization of types I, II, and X collagen in the tibial insertion sites of the medial meniscus. Knee Surg Sports Traumatol Arthrosc 2000;8:61–5.

[54] Kambic HE, McDevitt CA. Spatial organization of types I and II collagen in the canine meniscus. J Orthop Res 2005;23:142–9.

[55] de Mulder EL, Hannink G, Giele M, Verdonschot N, Buma P. Proliferation of meniscal fibrochondrocytes cultured on a new polyurethane scaffold is stimulated by TGF-ss. J Biomater Appl 2011.

[56] Kanazawa T, Furumatsu T, Hachioji M, Oohashi T, Ninomiya Y, Ozaki T. Mechanical stretch enhances COL2A1 expression on chromatin by inducing SOX9 nuclear translocation in inner meniscus cells. J Orthop Res 2012;30:468–74.

[57] Petri M, Ufer K, Toma I, Becher C, Liodakis E, Brand S, et al. Effects of perfusion and cyclic compression on in vitro tissue engineered meniscus implants. Knee Surg Sports Traumatol Arthrosc 2012;20:223–31.

[58] Adesida AB, Grady LM, Khan WS, Millward-Sadler SJ, Salter DM, Hardingham TE. Human meniscus cells express hypoxia inducible factor-1alpha and increased SOX9 in response to low oxygen tension in cell aggregate culture. Arthritis Res Ther 2007;9:R69.

[59] Saliken DJ, Mulet-Sierra A, Jomha NM, Adesida AB. Decreased hypertrophic differentiation accompanies enhanced matrix formation in co-cultures of outer meniscus cells with bone marrow mesenchymal stromal cells. Arthritis Res Ther 2012;14:R153.

[60] Ionescu LC, Lee GC, Huang KL, Mauck RL. Growth factor supplementation improves native and engineered meniscus repair in vitro. Acta Biomater 2012;8:3687–94.

[61] Mandal BB, Park SH, Gil ES, Kaplan DL. Stem cell-based meniscus tissue engineering. Tissue Eng A 2011;17:2749–61.

[62] Fox DB, Warnock JJ, Stoker AM, Luther JK, Cockrell M. Effects of growth factors on equine synovial fibroblasts seeded on synthetic scaffolds for avascular meniscal tissue engineering. Res Vet Sci 2010;88:326–32.

[63] Cucchiarini M, Schetting S, Terwilliger EF, Kohn D, Madry H. RAAV-mediated overexpression of FGF-2 promotes cell proliferation, survival, and alpha-SMA expression in human meniscal lesions. Gene Ther 2009;16:1363–72.

[64] Furumatsu T, Kanazawa T, Yokoyama Y, Abe N, Ozaki T. Inner meniscus cells maintain higher chondrogenic phenotype compared with outer meniscus cells. Connect Tissue Res 2011;52:459–65.

[65] Hellio Le Graverand MP, Ou Y, Schield-Yee T, Barclay L, Hart D, Natsume T, et al. The cells of the rabbit meniscus: their arrangement, interrelationship, morphological variations and cytoarchitecture. J Anat 2001;198:525–35.

[66] Melrose J, Smith S, Cake M, Read R, Whitelock J. Comparative spatial and temporal localisation of perlecan, aggrecan and type I, II and IV collagen in the ovine meniscus: an ageing study. Histochem Cell Biol 2005;124:225–35.

[67] Ochi M, Mochizuki Y, Deie M, Ikuta Y. Augmented meniscal healing with free synovial autografts: an organ culture model. Arch Orthop Trauma Surg 1996;115:123–6.

[68] Li S-T, Rodkey WG, Yuen D, Hansen P, Steadman JR. Type I collagen-based template for meniscus regeneration. In: Lewandrowski K-U, Wise DL, Trantolo DJ, Gresser JD, Yaszemski MJ, Altobelli DE, editors. Tissue engineering and biodegradable equivalents scientific and clinical applications. New York: Marcel Dekker; 2002. p. 237–66.

[69] Xia C, Fang NX. 3D microfabricated bioreactor with capillaries. Biomed Microdevices 2009;11:1309–15.

[70] Mishima Y, Lotz M. Chemotaxis of human articular chondrocytes and mesenchymal stem cells. J Orthop Res 2008;26:1407–12.